Genetic algorithm supported by influence lines and neural network for bridge health monitoring

Genetic algorithm supported by influence lines and neural network for bridge health monitoring

G. Marasco[1]; G. Piana[2,3]*; B. Chiaia[4]; and G. Ventura[5]

[1] Politecnico di Torino, Department of Structural, Geotechnical and Building Engineering, Corso Duca degli Abruzzi 24, 10129 Torino, Italy. E-mail: giulia.marasco@polito.it

[2] Politecnico di Torino, Department of Structural, Geotechnical and Building Engineering, Corso Duca degli Abruzzi 24, 10129 Torino, Italy. E-mail: gianfranco.piana@polito.it

[3] Tongji University, Department of Bridge Engineering, 1239 Siping Road, Shanghai, P.R. China. E-mail: gianfranco.piana@polito.it

[4] Politecnico di Torino, Department of Structural, Geotechnical and Building Engineering, Corso Duca degli Abruzzi 24, 10129 Torino, Italy. E-mail: bernardino.chiaia@polito.it

[5] Politecnico di Torino, Department of Structural, Geotechnical and Building Engineering, Corso Duca degli Abruzzi 24, 10129 Torino, Italy. E-mail: giulio.ventura@polito.it

ABSTRACT

The paper proposes a hybrid technique to solve the inverse problem of damage localization and severity estimation in beam structures. The first phase of the method involves the use of influence lines (IL) to extract information about the damage location. Then, a genetic algorithm (GA), representing the core of the whole procedure, utilizes static parameters as displacements and rotations at few points to evaluate the bending stiffness along the structure by updating a finite element model. The information obtained in the first phase is used in the second phase for: (i) reducing the number of design variables of the GA and the consequent computational time; (ii) improving the accuracy of GA solutions because it allows a suitably trained neural network to select proper values for the coefficients of the proposed cost function inside the genetic algorithm. The procedure is applied to a test problem, namely a simply supported, prestressed

concrete railway bridge, located in northern Italy. Numerical experiments are also conducted to test the procedure when the beam length and geometric properties vary.

Keywords: PC bridge; damage detection; influence line; neural network; genetic algorithm.

INTRODUCTION

In the last two decades, the need to control the safety of civil infrastructure facilities has become increasingly important. As proved also by recent happenings, the lack of knowledge of the actual structural conditions of structures and infrastructures and the consequent underrating of their vulnerability can imply severe problems. For example, structural damage due to corrosion, fatigue and aging can lead to significant losses, both in terms of human lives and economic resources. On the one hand, the development of a maintenance plan based on operations of detection, localization and quantification of damage is a complex task for engineers and infrastructure owners. On the other hand, the necessity of infrastructure managers to have a monitoring system that could be sustainable from an economic standpoint and able to point out the structural criticalities needs answers.

The state of the infrastructural asset is in continuous change due both to gradual (e.g. fatigue, corrosion) and shock (e.g. earthquakes, floods, and tornados) deterioration phenomena. Railway concrete bridges are subjected to several types of degradation mechanisms. The taxonomy (Maksymowicz et al. 2006) of the degradation processes and their classification highlight the main structural issues. They are due to deformation, discontinuity, displacement, loss of material, and deterioration (Bień et al. 2007). In detail, chemical (carbonation, salt, and acid actions) and physical (creep, fatigue, freeze-thaw action, overloading, shrinkage) phenomena can change structural features. Significant benefits are obtained from the acquisition of structural information to reduce the risk of human and economic losses. Some methods, e.g. Bayesian decision analysis (Iannacone et al. 2021), are useful to estimate them. On the other hand it is now well-known, and quantified by the De Sitter's "Law of five" (De Sitter 1984), the severe impact that a lack of maintenance can have on the overall costs. The recent happenings (Bazzucchi et al. 2018), including the

collapse of the Polcevera Viaduct in Genoa, Italy, have shown the need for effective control strategies to ensure safety in the infrastructural field (Clemente 2020).

Bridges structural evaluation based on non-destructive monitoring system (Kaloop et al. 2016) has been performed using both dynamic and static measurements. The first approach involves the use of vibrational measurements by means of operational modal analysis (OMA) and Experimental modal analysis (EMA) (Schwarz and Richardson 1999) to estimate the modal parameters and to track their evolutions. OMA is the most common procedure (Magalhães and Cunha 2011) as it does not require the use of any artificial excitation with consequent interruption of the facility operation. Dynamic methods in Structural Health Monitoring (SHM) have been investigated and developed for several decades and represent effective tools. The literature on the subject is very vast. Examples of data analysis from ambient vibration recording are reported in (Azzara et al. 2017)(Roselli et al. 2018)(Chiaia et al. 2020). At the same time, critical issues arise when using them for in-situ monitoring. In fact, damage detection based on the response in terms of frequencies (Salawu 1997), mode shapes (Allemang 2003), and damping ratios (Curadelli et al. 2008) has highlighted as factors like data volume, monitoring time, uncertainty (Reynders et al. 2008), and environmental effects have a significant impact on damage detection because they generate data variance (Wu et al. 2020). As a matter of fact, many novelty detection methods are not able to distinguish between frequency variations due to environmental/operational conditions and variations induced by a damage in the structure. It is true that methods exist for filtering data from disturbances, but this is not an easy operation and usually requires a long-term monitoring, and thus a lot of data to be stored. Progression to real-world applications is delayed by the shortcomings still present in addressing the negative effects produced by these factors (Moughty and Casas 2017). Furthermore, as in the case in matter, infrastructure managers experience difficulties in storing dynamic data from continuous monitoring and they require investigations that are able to exploit static data from periodic monitoring.

The second approach requires static load testing and collection of displacement (Nguyen et al. 2016), strain (Sanayei et al. 2012), and curvature (Tonnoir et al. 2018) data. The advantage in their use lies in a more direct achieving of the second level of the hierarchical structure into which the damage identification

problem can be divided, i.e. damage localization (Farrar and Worden 2012). In recent years, data-driven algorithms have been implemented within the SHM framework due to their ability in analyzing data and providing a real-time solution for decision making (Tibaduiza Burgos et al. 2020). Big data (BD) and Artificial Intelligence (AI) are considered promising approaches for an effective structural assessment (Sun et al. 2020). The applications of machine learning (Bao and Li 2020) and deep learning techniques (Toh and Park 2020) (Azimi et al. 2020) have been having a rapid increase and have been garnering a growing focus due to their better performance in a damage detection scenario (Flah et al. 2020). Therefore, investigations in this direction are of interest and new methodologies can assist more traditional ones like dynamic health monitoring, acoustic emission monitoring, etc.

The present work aims at investigating the possibility of using a reduced number of sensors/measure points while achieving satisfactory results in terms of damage identification at the same time. Structural assessment is designed as an outcome of a periodic (not continuous) monitoring in which few static parameters are recorded when a given external load acts in different positions over the structure. Comparing measurements made at different times under the same conditions can give information about possible changes in the structural response. For this purpose, the paper proposes a hybrid technique to solve the inverse problem of the damage localization and its severity estimation based on a genetic algorithm supported by influence lines and a neural network. The first phase involves the use of influence lines to extract information about the damage location (Chen et al. 2021). Then, a genetic algorithm (GA), representing the core of the whole procedure, utilizes static parameters measured at few points, i.e. mid-span deflections and end rotations, for estimating the bending stiffness along the discretized structure. The use of a limited number of parameters, distributed to capture potential changes both in the middle of the beam and near the supports, falls within an optimization perspective. Indeed, an increase in parameters would imply redundancy and greater reliability in the damage identification problem resolution but producing, on the other hand, an increase in cost and computational time. The information provided by the first phase yields two advantages: (1) it allows reducing the number of design variables of the algorithm and the consequent computational time; (2) it improves the accuracy of the solution given by the GA

because it allows a suitably trained neural network to find the best values of the coefficients of the GA's cost function. The use of a cost function composed by parts having different sensitivities to the damage locations gives the possibility to weight the different contributions by means of power coefficients.

To initially validate the overall approach (influence lines, genetic algorithm, and neural network) on an elementary test problem, the method is applied to a simply supported beam with damage scenarios characterized by localized reductions in the bending stiffness. To check the feasibility with actual values, model data refer to an existing prestressed concrete railway bridge, located in northern Italy. In addition, numerical experiments are conducted to test the procedure when the beam length and geometric properties are changed. Obtained results look promising and encourage further developments for an extension of the proposed method to more complex structural systems.

MOTIVATION AND PROBLEM DEFINITION

The methodology, although included in a general framework, was focused on a simply supported prestressed concrete railway bridge. Such choice is motivated by the fact that this type of viaduct represents most railway viaducts built in Italy since the second half of the 20th century. They suffer from a lot of damage phenomena, like transverse and longitudinal cracking, surface and internal humidity, water infiltration, defects in concrete along the cable track, and defects in prestressing cables. Fig. 1 shows some of the most important phenomena. As can be deduced, the severity of the deterioration can also be high, therefore causing considerable variations of the effective geometric properties of the beam cross-sections (e.g., bending rigidity).

The present work proposes a solution to address the damage detection problem in the framework of the structural health monitoring based on static measurements. The analysis focused on a specific bridge. Figs. 2a and b display a general view of the viaduct and a bottom view of the deck, respectively. The deck has a span of about 30 meters and is composed of four longitudinal prestressed beams, 2.5 meters deep, and five

diaphragms. The piers of the viaduct, having circular section with a diameter of 4 m, are connected at the top to a pier cap on which the beams lean against (Fig. 2).

In the structural design, the simultaneous presence of the LM71 (static vertical load of normal railway trains) and SW/2 (static load of heavy railway trains) on the two tracks was considered as the most severe condition for traffic loads. Figs. 3a and 3b display the longitudinal distribution of vertical loads for LM71 and SW/2, respectively. In the transverse direction, the design load distribution factors of LM71 lying on the left tracks are about 70% / 30% for the left inner / outer beam, respectively; and approximately 60% / 40% for the right inner / outer beam for SW/2 lying on the tracks on the right. Therefore, the left inner beam is the most loaded one (see Fig. 4).

Only the longitudinal flexural behavior was considered in this preliminary study. The single longitudinal beam-slab system (interior beam in Figure 4) was considered for the analyses. Its undamaged bending stiffness is $EI = 9.407\times10^{10}$ Nm^2 (Young's modulus $E = 36.28\times10^9$ N/m^2, area moment of inertia $I = 2.593$ m^4); the length is L=27.8 m. From the design report, it results a cracking bending moment equal to 31693.38 kNm (acting moment ad mid-span = 18209.80 kNm; safety factor = 1.7) and an ultimate resisting moment equal to 46200.39 kNm (acting moment at mid-span = 18209.80; safety factor = 2.5).

In the calculations, we considered a vertical travelling force whose magnitude, equal to 294.2 kN, is comparable to that of one of the concentrated loads in Figure 3a. It corresponds to the weight of a high-speed train bogie, providing a plausible force value for the test. The method can easily be extended to a series of travelling forces (train carriage).

METHODS

To analyze the damage scenarios, a finite element model (FEM) was used, with the beam discretized by *NE* = 27 beam elements (Fig. 5). We solved the structural problem by the implementing the displacement method based on the exact two-node beam stiffness matrix, which coincides with that of the two-node Euler-Bernoulli beam finite element. The solution in terms of nodal displacements is exact since nodal forces are considered; the deflection curve is sufficiently well described since element length is 1/27th of

154 the total beam length. We selected 27 elements for considering damages extending for a length of 1 m
155 (which is realistic in some cases; see Figure 1). Considering more elements would only increase the
156 computational effort, which however is rather small for a simple problem as the one under discussion.

157 Static deflection was chosen to assess the structural state (Chou and Ghaboussi 2001) because it is more
158 locally sensitive to damage than dynamic response. Moreover, static measurements are often easier to
159 perform and more precise than dynamic ones (Jenkins et al. 1997). The mid-span deflection and the
160 rotations at the two supports were taken as the reference quantities. The values of bending stiffness along
161 the structure, considered as unknowns, are calculated based on the measured and model computed quantities
162 in order to evaluate the structural conditions. The "measured" quantities (mid-span deflection or end
163 rotation), which should come from in-situ measurements in practice, were derived from the FEM model
164 corresponding to the imposed damage scenario in this analysis; they are input data. The model computed
165 quantities (mid-span deflection or end rotation) were those produced by the FEM model which uses the
166 trial bending stiffness values coming from the genetic algorithm. Thus, the unknown quantities, expressed
167 in this context by the values of bending stiffness, can be determined (estimated) by comparing measured
168 and computed quantities and looking for those values which minimize the difference between the two sets
169 of data.
170 The structural assumptions and the main steps of the proposed methodology, that will be explained in detail
171 in the following sections, are summarized in the flowchart displayed in Fig. 6.

172

173 **Damage localization: influence line method**

174 As is well known, influence lines give the value at a *particular* point in a structure of entities such as shear
175 force, bending moment, support reaction, displacement and rotation for *all* positions of a travelling unit
176 load. The presence of damage in beams (Chen et al. 2014; Štimac et al. 2006) can be observed and localized
177 utilizing influence lines (Megson 2019). For example, let $\eta_m(x)$ and $\bar{\eta}_m(x)$ be the displacement influence
178 lines at mid-span of the damaged and undamaged structures, respectively, i.e., the mid-point displacement

in the two structures when a travelling unit transverse force is acting at section *x*. Thus, the difference $\delta_m^{\eta}(x) = abs(\eta_m(x) - \bar{\eta}_m(x))$ will be larger at sections $x = x_d$ where a damage is present. Rotations or curvatures influence lines may be used in the same way (Štimac et al. 2006). This allows identifying the sections with possible damage, and also to investigate damage evolution by comparing measurements made at different times.

As an illustrative example, let us consider a simply supported beam, 10 m long, with undamaged bending rigidity EI = 1 Nm^2. Assume that the beam is discretized into 20 elements, 0.5 m long each, and that a damage is present in the fifth one (from the left) producing a 10% reduction in its bending rigidity, i.e. EI_d = 0.9 Nm^2. Influence lines can be calculated under the action of a travelling unit transverse force for the undamaged and damaged conditions. Fig. 7a shows, from left to right, the mid-span displacement influence line for the damaged beam, for the integer structure, and their difference as functions of the abscissa (load position). Similarly, Fig. 7b shows, from left to right, the left-support rotation influence line for the damaged beam, for the integer structure, and their difference as functions of the abscissa (load position). As can easily be seen, the diagrams of the difference show a maximum in correspondence to the damaged element, according with the discretization adopted.

Estimation of damage severity: genetic algorithm

The genetic algorithm (GA) is an optimization technique based on Darwinian principles (Mahalakshmi et al. 2013; Mirjalili et al. 2020) that allows the generation of good solutions starting from a population of individuals (often generated randomly) that evolve over time. After defining a set of possible solutions, namely a population of *npop* individuals, each solution is evaluated using a cost function. By using crossover and mutation operators, the better individuals are chosen to create new individuals (offsprings). Individuals' merge and sort operations are performed at this point, based on their cost function. The new generation will be made up of the better *npop* individuals. When the specified number of iterations is reached or the quality of the better solution is considered to be acceptable, the process is complete. Only

the most "suitable" individuals survive and replicate, reducing the cost of future generations. A lot of damage identification problems have been addressed in the scientific literature by exploiting this approach. Most of the investigations have been based on the comparison between the computed and the measured dynamic response (Au et al. 2003; Buezas et al. 2011; Hao and Xia 2002; Khatir et al. 2016; Meruane and Heylen 2011; Nobahari and Seyedpoor 2011). They use the natural frequencies and mode shapes of several vibration modes. Although effective, they imply the use of many sensors and a large volume of data. Studies which combine both static and dynamic characteristics (Jung and Kim 2013) point out an improvement of the results. The combination of modal parameters and static displacements (Jung and Kim 2013) (He and Hwang 2006), as well as the use of static response exclusively (He and Hwang 2007), is less common.

For the particular issue, in the present study individuals are constituted by the bending stiffness of the elements which were identified as damaged by the influence lines. Thus, the genetic algorithm, using the available static measurements, calculates the bending stiffness of the damaged elements once their location and number are known.

Design of genetic algorithm

The architecture of the GA requires the definition of several parameters, which are both “qualitative” and “quantitative” (Eiben and Smit 2011). The selection, crossover, and mutation operators are examples of the former type. The population size (*npop*), the crossover rate (*CR*), and the mutation rate (*MR*) belong to the latter type. The first set of parameters, known as high-level parameters, defines the algorithm's key structure: in this study, the Roulette Wheel Selection and the Uniform Crossover were the selected operators. The second set of parameters, known as low-level parameters, are used to create a version of the algorithm: they were determined as will be described later on.

Cost function

The GA's cost function is based on static parameters as mid-span displacement and support rotations. The construction of a cost function based exclusively on static measurements, able to exploit only three

measured values thus eliminating the need to accumulate large volume of data, is one of the distinctive features of the proposed approach. It is made of the sum of five contributions:

$$Cost = {Cost_{Disp_{pol}}}^{\rho} + {Cost_f}^{\varphi} + {Cost_{RotA}}^{\alpha 1} + {Cost_{RotB}}^{\alpha 2} + {Cost_{RatioRot}}^{\delta} \quad (1)$$

Power coefficients $\rho, \varphi, \alpha 1, \alpha 2$, and δ are introduced to weight the single contributions, which can be more or less sensitive to damage location. Their influence will be assessed in the following sections. Usually, they are initially set equal to one for preliminary analysis, and then computed at a later stage to improve the goodness of the solution, if necessary.

The expressions of each of the five contributions in Eq. (1) are the following (Eqs. (2-6)):

$${Cost_{Disp_{pol}}}^{\rho} = \left((NE-2)\frac{\sum abs(Disp_a - Disp_m)}{\sum abs(Disp_m)}\right)^{\rho} \quad (2)$$

$${Cost_f}^{\varphi} = \left(abs\left(\frac{f_m - f_a}{f_m}\right)\right)^{\varphi} \quad (3)$$

$${Cost_{RotA}}^{\alpha 1} = \left(abs\left(\frac{RotA_m - RotA_a}{RotA_m}\right)\right)^{\alpha 1} \quad (4)$$

$${Cost_{RotB}}^{\alpha 2} = \left(abs\left(\frac{RotB_m - RotB_a}{RotB_m}\right)\right)^{\alpha 2} \quad (5)$$

$${Cost_{RatioRot}}^{\delta} = \left(abs(Ratio_m - Ratio_a)\right)^{\delta} \quad (6)$$

Eqs. (7) and (8) show the expressions adopted for $Ratio_m$ and $Ratio_a$, respectively:

$$Ratio_m = abs\left(\frac{RotA_m}{RotB_m}\right), \quad (7)$$

$$Ratio_a = abs\left(\frac{RotA_a}{RotB_a}\right). \quad (8)$$

The terms $Cost_f{}^{\varphi}$, $Cost_{RotA}{}^{\alpha 1}$, and $Cost_{RotB}{}^{\alpha 2}$ are directly linked to the measurements made (displacement at mid-span and rotations at supports *A* and *B*). The first term, $Cost_{Disp_{pol}}{}^{\rho}$, is stemmed from the displacements of the other structural nodes, which are estimated using the Vurpillot algorithm starting from the measured quantities; the differences between computed and measured quantities which appear in the numerator are normalized with respect to the average measured displacement. The last term, $Cost_{RatioRot}{}^{\delta}$, is based on the ratio between the rotations at the supports. Subscripts *m* and *a* denote measured and analytical (computed) quantities, respectively. The measured values were numerically simulated using a FEM analysis, with the damaged elements having a reduced bending stiffness, as previously mentioned; in real-world application, they should come from on-site measurements. The analytical quantities, on the other hand, were determined using a FEM analysis in which the values of bending stiffness of the damaged elements were picked-up from the GA individuals. The power coefficients for each part of the cost function were set equal to 1 at the beginning.

Advantages coming from the use of such a cost function include: (i) utilizing few sensors/measure points (thanks to the form of the cost function and information provided by influence lines); (ii) inclusion of parameters as end rotations which are usually not considered; (iii) no need to save big volumes of data; (iv) reduced computational time.

Preliminary study: tuning of the numerical parameters of GA

Each quantitative hyperparameter utilized within the genetic algorithm has a specific influence (Hassanat et al. 2019) and a great impact on its performance. Consequently, it is not appropriate to recklessly proceed with their selection.

Along with the previously described parameters (*npop, CR, MR*), there are three additional ones (β, γ, σ) that depend on the chosen operators and deserve further exploration. The first one, β, allows the Roulette Wheel method to select the parents by assigning probabilities (*probs*) to the individuals of the population. This approach is carried out by defining a probability distribution over the population in a way such that the better individuals of the population have a higher chance of being selected as parents.

$$probs = e^{-\beta c} \quad (9)$$

The symbol *c*, used in Eq. (9), represents the cost of the individual normalized with respect to the average cost of the population.

The second hyperparameter, γ, is related to the uniform crossover operator. It increases the exploration capabilities of the GA. A couple of offsprings y_j (*j*=1,2) with *n* genes (Eq. (11)) is built starting from a couple of parents x_j (j=1,2) with *n* genes (Eq. (10)). The *i*-th genes of the *j*-th offspring (Eq. (12)) is linked to the *i*-th gene of the corresponding parent (x_{ji}) and to the i-th gene of the other ($x_{\bar{j}i}$) by means of the parameter α_i. The γ parameter is used to extend the classical dispersion range of α_i from [0, 1] to [$-\gamma$, $1+\gamma$]. In this way, it is possible to create offspring somehow different from their parents.

$$x_j = (x_{j1,}x_{j2}, \dots\dots, x_{jn}) \quad (10)$$

$$y_j = \left(y_{j1,}y_{j2}, \dots\dots, y_{jn}\right) \quad (11)$$

$$y_{ji} = \alpha_i x_{ji} + (1 - \alpha_i)x_{\bar{j}i} \quad (12)$$

The third hyperparameter, σ, is related to the mutation operator. Such operation occurs by adding a random number with zero mean and variance σ^2.

In the general context of a grid search strategy (Pontes et al. 2016; RAMADHAN et al. 2017; Shekar and Dagnew 2019), a complete search was performed on a subset of the space of hyperparameters defined in Tab.1. This latter gives details on the range values and step used for each of them.

Neural network: supervised learning for selection of cost function power coefficients

A neural network, namely a supervised learning model nowadays successful in many scientific fields (Abiodun et al. 2018), was used to improve accuracy (and consequently decrease the error) of the solutions provided by the genetic algorithm. It was trained to select suitable power coefficients for the cost function, once the damaged elements were localized. Numerical simulations were carried out to associate the damage scenarios, characterized by some damaged elements, to the power coefficients. Several damage cases were investigated and, for each of them, numerical analyses considering 10,000 combinations of power

coefficients were performed. The minimum and the maximum values of the investigated variability range for each power coefficient were set equal to 0.1 and 1, respectively; the step was set to 0.1. The only exception was made for ρ. Since the corresponding term in the cost function is linked to computed parameters rather than measured ones, this coefficient was set to 1. For each damage scenario, the combination of power coefficients corresponding the least error was chosen among the 10,000 ones. In this analysis, the error was defined as the absolute value of the difference between the genetic algorithm's solution and the correct value of the variables. Further connections between other cases of damage and power coefficients were built using a simplified method due to the high computational and time effort involved in this procedure (Bergstra and Bengio 2012; Fayed and Atiya 2019; Huang et al. 2012; Shekar and Dagnew 2019; Syarif et al. 2016). For damage cases similar to the ones already considered, where similar means that the positions of the damages are near to the ones just analyzed, the power coefficients previously calculated with the addition of a noise were utilized. The added noise ranges from 0.5% to 1.5% based on the greater or lesser proximity to the previously investigated case. A neural network was trained and tested using the 171 connections created. Its structure is depicted in Fig. 8. Every example fed into the neural network has seven inputs. The first five are reserved for indicating damaged elements, which were marked by a number ranging from 1 to 27. If the number of damaged elements, *nd*, is less than 5, the remaining 5–*nd* inputs are given a zero value. The positions of the most affected elements are included in the last two inputs. The targets, on the other hand, are made up of the four power coefficients.

The samples were subdivided into three parts: training (70%), validation(15%) and testing (15%). A two-layer feedforward network, with a sigmoid transfer function in the hidden layer and a linear transfer function in the output layer, was employed. The number of hidden neurons was set to 27, and the training algorithm used Bayesian regularization. Regression value, *R*, and Mean Squared Error, *MSE*, were used to evaluate the performance. *R* measures the correlation between outputs and targets. Values of *R* close to 1 indicate close relationship, whereas values close to 0 indicate random relationship. The Mean Squared Error

is the avearge square difference between outputs and targets. Low values of this index indicate a good performance.

RESULTS

The influence lines of mid-span deflection and support rotations under the above-mentioned travelling force were numerically computed for the undamaged and damaged structures for the problem in exam. This allowed the damaged elements in the discretized structure parameter to be identified, providing information for the genetic algorithm.

Fig. 9 shows three structural damage scenarios with two damaged elements. The upper part of the figure displays the structural schemes. The most severely damaged element, and the associated flexural stiffness, is highlighted in red. Orange color is used for the element with less severe damage. For example, the case on the right has two damaged elements, one with a 0.9*EI* for element n. 7 (*de* = 7) and the other with a 0.75*EI* for element n. 16 (*de* = 16). The squares of relative differences $\delta_m^{\eta,rel}$, $\delta_A^{\varphi,rel}$ and $\delta_B^{\varphi,rel}$ for the mid-span displacement, the left (*A*) and right (*B*) support rotations (e.g. $\delta_m^{\eta,rel} = abs((\eta_m(x) - \bar{\eta}_m(x))/\bar{\eta}_m(x))$ show peaks (diamonds) in correspondence to the damaged elements. The use of these three indices also makes it possible to localize damage even in regions, like those near the supports, for which is usually difficult (see the second case in Fig. 9).

It is worth noting that the selected bridge has a relatively high bending stiffness. Under the applied travelling force, this resulted in very small variations in the values of displacement and rotation between the undamaged and damaged states. However, high-sensitivity displacement transducers, such as LVDT sensors, as well as modern techniques such as Digital Image Correlation (DIC) (Lacidogna et al. 2020), are now available for micrometer measurements. Other damage-sensitive mechanical quantities, such as strains, may also be used, the technique still being accurate and the above-described procedure remaining unvaried in principle. The operation of damage localization performed by the influence lines results effective for the subsequent estimation of damage severity. Performing these two operations simultaneously

would turn out to be a process with a high computational cost, especially for complex problems. In these cases, in fact, the number of design variables is high and the accuracy of the solution decays. Influence lines not only exclude from further analysis those elements with a low probability of damage, as it occurs in grey relation analysis (He and Hwang 2007), but are also able to drastically reduce the number of design variables by identifying damaged elements. The use of influence lines applied to the simple beam structure is a simplification that has allowed a first validation of the procedure. To better describe the structural behavior of the bridge, influence surfaces should be used on a 2D structural model (Štimac et al. 2006).

As previously pointed-out, a preliminary study was conducted for tuning the numerical parameters of the GA. The goal of this preliminary analysis was not to find the best combination of hyperparameters, but rather the combination that produce suitable results for subsequent studies. Thus, the comparison among the performances in terms of cost, for each structural problem (case of damage) and each combination of parameters, was carried out ignoring the stochastic nature of the problem. A total of 8400 combinations of parameters were generated by using the range values and steps in Tab. 1.

The behavior of the cost function with respect to the combination of parameters was observed for each of the four investigated damage cases (DC). For simplicity, in each case only one damaged element is present in the structure. Therefore, the number of the variables within the GA was set equal to one. Tab. 2 reports, for the four examined damage cases, the number *de* (comprised between 1 and 27, starting from the left support A) that identifies the damaged element, and the corresponding bending stiffness, EI_d, expressed as a fraction of the undamaged bending stiffness *EI*. Fig. 10 shows the cost as a function of the combinations of parameters and damage scenarios DC_1 to DC_4. The cost resulted to be highly sensitive to the used parameters, especially for DC_1. Thus, referring to DC_1 as the worst case, the combination of parameters that corresponds to the minimum cost was chosen, i.e. combination 558; see Tab. 3.

For the examined damage scenarios, the results in terms of cost, accuracy, and error are collected in Tab. 4. The accuracy was computed as the ratio between the computed solution and the correct value. The error was calculated as follows:

$$Error = \frac{GA\_value - Correct\_value}{Correct\_value} \quad (13)$$

The findings might be deemed acceptable, but they are still subject of improvement. For this purpose, the impact of the power coefficients φ, $\alpha 1$, $\alpha 2$, δ of the cost function, up to now considered unitary, was investigated starting from the knowledge of the damage location. After having found the benefits obtainable from the variation of these coefficients in the simplest damage scenario (only one damaged element), it was considered appropriate to fully exploit the information related to the location of the damage to obtain better results also in the most complex damage scenarios.

By exploiting the neural network as previously described, a value of regression *R* of about 0.92 for the training set and about 0.88 for the test set were obtained. They may be judged as satisfactory, although of course they can still be improved by increasing the number of sample cases used to train the network. Recent studies focused on the investigation of the effects of varying the number of train samples for a fixed model and a training samples have shown that by drastically increasing the number of training samples with respect to the complexity of the model, it is possible to decrease the error on the test (Nakkiran and Yang 2018).

Fig. 11 (right) shows the value of *MSE* for the training and test sets vs. the variation of the epochs. The best value of *MSE* was reached by the training set at epoch 1000 and it is fairly small. Besides, the downward trend of the *MSE* index for the test set indicates that there is no overfitting of the training data. By overcoming the overfitting process, an increase in the number of epochs could boost the network's efficiency even further (Nakkiran and Yang 2018). Another method for measuring the network's goodness is the error histogram shown in Fig. 11 (left). We can see that the error follows a Gaussian distribution with a mean close to zero and a slight dispersion.

A series of validation tests were performed to verify the NN's robustness in generating power coefficients that allow an accurate damage severity estimation. Starting from new damage cases, assumed known the damage location from the influence line method, the neural network was used to produce the power

coefficients to be introduced into the genetic algorithm for the estimation of the bending stiffness of the damaged elements. Tab. 5 contains the findings for one of the new damage cases tested. The error in estimating the bending stiffness was calculated by Eq. (13).

The error distribution is depicted in Fig. 12. The normal distribution, with a mean equal to –0.011 and a standard deviation equal to 0.06, points out that about the 70% of damage cases has an error less than 6%. In the same figure, the logistic distribution is also used to fit the data. With a mean of –0.0026 and a standard deviation of 0.025, it seems to fit the data even better. The damaged cases in Fig. 12 are those showing the largest errors. In general, the findings are thus considered satisfactory and still improvable by training the NN with more cases in order to remove the tails of the probability distribution.

The same damage cases were used to test the actual improvement in results which can be obtained, with the approach described so far, by using power coefficients extracted from the neural network. Using unitary coefficients, a normal distribution of the error was obtained with a mean of –0.015 and a standard deviation of 0.48, i.e. a less accurate solution compared to the above results. The approach is therefore valid.

Moreover, the same damage scenarios were used to test the validity of the methodology as the geometric properties of the beam are changed. For example, if a beam length of 50 meters is considered, the error distribution remains essentially unchanged. Also, even by varying the value of the moment of inertia I, the distributions undergo very slight changes. Results for moment of inertia values of 2 and 1.5 m^4 were investigated. In these cases, the mean of the normal distribution is about –0.01, with a standard deviation of about 0.08. These results are encouraging about the validity of the methodology as the geometric properties of the beam vary.

Lastly, we underline that the methodology results sustainable also from a computational point of view. The required computational time is in fact equal to about 2.5 seconds for each analysis involving the genetic algorithm.

CONCLUSIONS

418 The paper aimed at exploring the potential of a hybrid technique based on static measurements which can
419 help a genetic algorithm to identify and quantify damage in structures using a reduced number of variables.
420 A simply supported beam problem was selected to initially test the method, with data taken from a real
421 bridge structure for checking its effectiveness with actual values. The proposed hybrid technique for the
422 inverse problem of damage identification (detection, localization and estimation) has proven to be
423 successful and promising. The main new features and the associated advantages can be summarized as
424 follows:

425 • The use of influence lines with the three associated indices – namely, the square of relative
426 differences between undamaged and damaged stages for the mid-span displacement, $\left(\delta_m^{\eta,rel}\right)^2$, and
427 the left (*A*) and right (*B*) support rotations, $\left(\delta_A^{\varphi,rel}\right)^2$ and $\left(\delta_B^{\varphi,rel}\right)^2$ – makes it possible to identify
428 damaged regions (beam elements), either along the span or near the supports.

429 • The use of influence lines sharply reduces the design variables of the genetic algorithm by
430 overcoming the concept of excluding unlikely damage locations (e.g. grey relation analysis). In this
431 way the computational time drops.

432 • The use of a cost function expressed as the sum of five addends, more or less influenced by the
433 damage according to its location, allows to associate a specific weight to each of them by means of
434 power coefficients and to improve the accuracy (decrease the error) of the solution. Results show
435 that, in the analyzed case, very good predictions are obtained adopting three measure
436 points/sensors. Displacements at any node used in the cost function are calculated starting from the
437 values of the mid-span displacement and the two end rotations only.

438 • The trained neural network turns out to be an effective support to set the power coefficient of the
439 cost function. Its architecture can also encompass cases with more than two damaged elements.

- Here, the approach was positively tested on a simply supported beam with damage scenarios defined by localized bending stiffness reductions. The same damage scenarios were used to test the validity of the methodology when the beam length and geometric properties are varied: good results were obtained without changing the coefficients in the algorithm.

Summarizing, the obtained advantages are in terms of computational time, location of critical elements using few measure points, and versatility of the approach. The satisfactory results obtained for the analyzed case make this approach appealing and worthy of further deepening. Although further work is to be done before moving to real-world application, the proposed method is amenable to generalization. In this direction, planned future developments go toward the use of more refined structural models (grillage) as well as the use of influence surfaces for damage localization, other damage indicators, and the analysis of different damage scenarios.

Data Availability

Some or all data, models or code that support the findings of this study are available from the corresponding author upon reasonable request.

References

Abiodun, O. I., Jantan, A., Omolara, A. E., Dada, K. V., Mohamed, N. A., and Arshad, H. (2018). "State-of-the-art in artificial neural network applications: A survey." *Heliyon*, Elsevier, 4(11), e00938.

Allemang, R. J. (2003). "The modal assurance criterion–twenty years of use and abuse." *Sound and vibration*, Citeseer, 37(8), 14–23.

Au, F. T. K., Cheng, Y. S., Tham, L. G., and Bai, Z. Z. (2003). "Structural damage detection based on a micro-genetic algorithm using incomplete and noisy modal test data." *Journal of Sound and Vibration*, Elsevier, 259(5), 1081–1094.

Azimi, M., Eslamlou, A. D., and Pekcan, G. (2020). *Data-driven structural health monitoring and damage detection through deep learning: State-ofthe- art review*. *Sensors (Switzerland)*.

Azzara, R. M., De Falco, A., Girardi, M., and Pellegrini, D. (2017). "Ambient vibration recording on the Maddalena Bridge in Borgo a Mozzano (Italy): data analysis." *Annals of Geophysics*.

Bao, Y., and Li, H. (2020). "Machine learning paradigm for structural health monitoring." *Structural Health Monitoring*, SAGE Publications Sage UK: London, England, 1475921720972416.

Bazzucchi, F., Restuccia, L., and Ferro, G. A. (2018). "Considerations over the Italian road bridge infrastructure safety after the Polcevera viaduct collapse: past errors and future perspectives." *Frattura e Integrita Strutturale*, 12.

Bergstra, J., and Bengio, Y. (2012). "Random search for hyper-parameter optimization." *Journal of machine learning research*, 13(2).

Bień, J., Jakubowski, K., Kamiński, T., Kmita, J., Kmita, P., Cruz, P. J. S., and Maksymowicz, M. (2007). "Railway bridge defects and degradation mechanisms."

Buezas, F. S., Rosales, M. B., and Filipich, C. P. (2011). "Damage detection with genetic algorithms taking into account a crack contact model." *Engineering Fracture Mechanics*, Elsevier, 78(4), 695–712.

Chen, Z., Cai, Q., Lei, Y., and Zhu, S. (2014). "Damage detection of long-span bridges using stress influence lines incorporated control charts." *Science China Technological Sciences*, Springer, 57(9), 1689–1697.

Chen, Z. W., Zhao, L., Zhang, J., Cai, Q. L., Li, J., and Zhu, S. (2021). "Damage quantification of beam structures using deflection influence line changes and sparse regularization." *Advances in Structural Engineering*, (422).

Chiaia, B., Marasco, G., Ventura, G., and Zannini Quirini, C. (2020). "Customised active monitoring

487 system for structural control and maintenance optimisation." *Journal of Civil Structural Health*
488 *Monitoring*, Springer Berlin Heidelberg, 10(2), 267–282.

489 Chou, J. H., and Ghaboussi, J. (2001). "Genetic algorithm in structural damage detection." *Computers*
490 *and Structures*, 79(14), 1335–1353.

491 Clemente, P. (2020). "Monitoring and evaluation of bridges: lessons from the Polcevera Viaduct collapse
492 in Italy." *Journal of Civil Structural Health Monitoring*, Springer.

493 Curadelli, R. O., Riera, J. D., Ambrosini, D., and Amani, M. G. (2008). "Damage detection by means of
494 structural damping identification." *Engineering Structures*, Elsevier, 30(12), 3497–3504.

495 Eiben, A. E., and Smit, S. K. (2011). "Parameter tuning for configuring and analyzing evolutionary
496 algorithms." *Swarm and Evolutionary Computation*, Elsevier, 1(1), 19–31.

497 Farrar, C. R., and Worden, K. (2012). *Structural health monitoring: a machine learning perspective*. John
498 Wiley & Sons.

499 Fayed, H. A., and Atiya, A. F. (2019). "Speed up grid-search for parameter selection of support vector
500 machines." *Applied Soft Computing*, Elsevier, 80, 202–210.

501 Flah, M., Nunez, I., Ben Chaabene, W., and Nehdi, M. L. (2020). "Machine Learning Algorithms in Civil
502 Structural Health Monitoring: A Systematic Review." *Archives of Computational Methods in*
503 *Engineering*, Springer Netherlands, (0123456789).

504 Hao, H., and Xia, Y. (2002). "Vibration-based damage detection of structures by genetic algorithm."
505 *Journal of computing in civil engineering*, American Society of Civil Engineers, 16(3), 222–229.

506 Hassanat, A., Almohammadi, K., Alkafaween, E., Abunawas, E., Hammouri, A., and Prasath, V. B. S.
507 (2019). "Choosing mutation and crossover ratios for genetic algorithms-a review with a new
508 dynamic approach." *Information (Switzerland)*, 10(12).

He, R.-S., and Hwang, S.-F. (2006). "Damage detection by an adaptive real-parameter simulated annealing genetic algorithm." *Computers & Structures*, Elsevier, 84(31–32), 2231–2243.

He, R.-S., and Hwang, S.-F. (2007). "Damage detection by a hybrid real-parameter genetic algorithm under the assistance of grey relation analysis." *Engineering Applications of Artificial Intelligence*, Elsevier, 20(7), 980–992.

Huang, Q., Mao, J., and Liu, Y. (2012). "An improved grid search algorithm of SVR parameters optimization." *2012 IEEE 14th International Conference on Communication Technology*, IEEE, 1022–1026.

Iannacone, L., Francesco Giordano, P., Gardoni, P., and Pina Limongelli, M. (2021). "Quantifying the value of information from inspecting and monitoring engineering systems subject to gradual and shock deterioration." *Structural Health Monitoring*, SAGE Publications Sage UK: London, England, 1475921720981869.

Jenkins, C. H., Kjerengtroen, L., and Oestensen, H. (1997). "Sensitivity of Parameter Changes in Structural Damage Detection." *Shock and Vibration*, IOS Press, 4, 27–37.

Jung, D. S., and Kim, C. Y. (2013). "Finite element model updating of a simply supported skewed PSC I-girder bridge using Hybrid Genetic Algorithm." *KSCE Journal of Civil Engineering*, 17(3), 518–529.

Kaloop, M. R., Hu, J. W., and Elbeltagi, E. (2016). "Evaluation of high-speed railway bridges based on a nondestructive monitoring system." *Applied Sciences*, Multidisciplinary Digital Publishing Institute, 6(1), 24.

Khatir, A., Tehami, M., Khatir, S., and Abdel Wahab, M. (2016). "Multiple damage detection and localization in beam-like and complex structures using co-ordinate modal assurance criterion combined with firefly and genetic algorithms." *Journal of Vibroengineering*, JVE International Ltd.,

18(8), 5063–5073.

Lacidogna, G., Piana, G., Accornero, F., and Carpinteri, A. (2020). “Multi-technique damage monitoring of concrete beams: acoustic emission, digital image correlation, dynamic identification.” *Construction and Building Materials*, Elsevier, 242, 118114.

Magalhães, F., and Cunha, A. (2011). “Explaining operational modal analysis with data from an arch bridge.” *Mechanical systems and signal processing*, Elsevier, 25(5), 1431–1450.

Mahalakshmi, M., Kalaivani, P., and Nesamalar, E. K. (2013). “A review on genetic algorithm and its applications.” *International Journal of Computing Algorithm*, 2(2), 415–423.

Maksymowicz, M., Cruz, P. J. S., Bień, J., and Helmerich, R. (2006). “Concrete railway bridges: Taxonomy of degradation mechanisms and damages identified by NDT methods.” Taylor & Francis.

Megson, T. H. G. (2019). *Structural and stress analysis*. Butterworth-Heinemann.

Meruane, V., and Heylen, W. (2011). “An hybrid real genetic algorithm to detect structural damage using modal properties.” *Mechanical Systems and Signal Processing*, Elsevier, 25(5), 1559–1573.

Mirjalili, S., Dong, J. S., Sadiq, A. S., and Faris, H. (2020). “Genetic algorithm: Theory, literature review, and application in image reconstruction.” *Nature-inspired optimizers*, Springer, 69–85.

Moughty, J. J., and Casas, J. R. (2017). “A state of the art review of modal-based damage detection in bridges: Development, challenges, and solutions.” *Applied Sciences*, Multidisciplinary Digital Publishing Institute, 7(5), 510.

Nakkiran, P., and Yang, T. (2018). “D EEP D OUBLE D ESCENT :” 1–24.

Nguyen, V. H., Schommer, S., Maas, S., and Zürbes, A. (2016). “Static load testing with temperature compensation for structural health monitoring of bridges.” *Engineering Structures*, Elsevier, 127,

554 700–718.

555 Nobahari, M., and Seyedpoor, S. M. (2011). “Structural damage detection using an efficient correlation-
556 based index and a modified genetic algorithm.” *Mathematical and Computer modelling*, Elsevier,
557 53(9–10), 1798–1809.

558 Pontes, F. J., Amorim, G. F., Balestrassi, P. P., Paiva, A. P., and Ferreira, J. R. (2016). “Design of
559 experiments and focused grid search for neural network parameter optimization.” *Neurocomputing*,
560 Elsevier, 186, 22–34.

561 RAMADHAN, M. M., SITANGGANG, I. S., NASUTION, F. R., and GHIFARI, A. (2017). “Parameter
562 Tuning in Random Forest Based on Grid Search Method for Gender Classification Based on Voice
563 Frequency.” *DEStech Transactions on Computer Science and Engineering*, (cece).

564 Reynders, E., Pintelon, R., and De Roeck, G. (2008). “Uncertainty bounds on modal parameters obtained
565 from stochastic subspace identification.” *Mechanical systems and signal processing*, Elsevier, 22(4),
566 948–969.

567 Roselli, I., Malena, M., Mongelli, M., Cavalagli, N., Gioffrè, M., De Canio, G., and de Felice, G. (2018).
568 “Health assessment and ambient vibration testing of the ‘Ponte delle Torri’ of Spoleto during the
569 2016–2017 Central Italy seismic sequence.” *Journal of Civil Structural Health Monitoring*,
570 Springer, 8(2), 199–216.

571 Salawu, O. S. (1997). “Detection of structural damage through changes in frequency: a review.”
572 *Engineering structures*, Elsevier, 19(9), 718–723.

573 Sanayei, M., Phelps, J. E., Sipple, J. D., Bell, E. S., and Brenner, B. R. (2012). “Instrumentation,
574 nondestructive testing, and finite-element model updating for bridge evaluation using strain
575 measurements.” *Journal of bridge engineering*, American Society of Civil Engineers, 17(1), 130–
576 138.

Schwarz, B. J., and Richardson, M. H. (1999). “Experimental modal analysis.” *CSI Reliability week*, Orlando FL, 35(1), 1–12.

Shekar, B. H., and Dagnew, G. (2019). “Grid search-based hyperparameter tuning and classification of microarray cancer data.” *2019 2nd International Conference on Advanced Computational and Communication Paradigms, ICACCP 2019*, IEEE.

De Sitter, W. R. (1984). “Costs of service life optimization" The Law of Fives".” *CEB-RILEM Workshop on Durability of Concrete Structures (Copenhagen, Denmark, May 18-20, 1983)*, Comité Euro-International du Béton, 131–134.

Štimac, I., Mihanović, A., and Kožar, I. (2006). “„Damage Detection from Analysis of Displacement Influence Lines “.” *International Conference on Bridges, Dubrovnik*, 1001–1008.

Sun, L., Shang, Z., Xia, Y., Bhowmick, S., and Nagarajaiah, S. (2020). “Review of Bridge Structural Health Monitoring Aided by Big Data and Artificial Intelligence: From Condition Assessment to Damage Detection.” *Journal of Structural Engineering*, 146(5), 04020073.

Syarif, I., Prugel-Bennett, A., and Wills, G. (2016). “SVM parameter optimization using grid search and genetic algorithm to improve classification performance.” *Telkomnika*, Ahmad Dahlan University, 14(4), 1502.

Tibaduiza Burgos, D. A., Gomez Vargas, R. C., Pedraza, C., Agis, D., and Pozo, F. (2020). *Damage identification in structural health monitoring: A brief review from its implementation to the use of data-driven applications*. *Sensors (Switzerland)*.

Toh, G., and Park, J. (2020). “Review of vibration-based structural health monitoring using deep learning.” *Applied Sciences (Switzerland)*, 10(5).

Tonnoir, B., Carde, C., and Banant, D. (2018). “Curvature: An Indicator of the Mechanical Condition of Old Prestressed Concrete Bridges.” *Structural Engineering International*, Taylor & Francis, 28(3),

357–361.

Wu, C., Wu, P., Wang, J., Jiang, R., Chen, M., and Wang, X. (2020). “Critical review of data-driven decision-making in bridge operation and maintenance.” *Structure and Infrastructure Engineering*, Taylor & Francis, 0(0), 1–24.

Table 1. Grid search for hyperparameter optimization.

Parameter	**Range**	**Step**
n_{pop}	[10-50]	20
CR	[0.5-1]	0.15
MR	[0.01-0.1]	0.02
β	[0.8-2]	0.2
γ	[0.1-0.5]	0.1
σ	[0.1-40]	10

Table 2. Damage scenarios.

	DC_1	DC_2	DC_3	DC_4
de	14	14	2	2
EI_d	*0.5EI*	*0.8EI*	*0.5EI*	*0.8EI*

Table 3. Chosen combination of parameters.

Combination 558					
n_{pop}	CR	MR	β	γ	σ
50	0.8	0.03	1.4	0.2	0.1

Table 4. Cost and accuracy with combination 558.

	DC_1	DC_2	DC_3	DC_4
Cost	0.59	0.30	0.24	0.29
Accuracy	1.00	0.91	1.00	1.00
Error	0	-0.09	0	0

Table 5. Example of new case of damage.

Damage case			
de	***EI$_d$***	***de***	***EI$_d$***
10	*0.8EI*	27	*0.95EI*
Power coefficients			
φ	***α$_1$***	***α$_2$***	***δ***
0.75	1.07	0.36	0.52
Error			
1.32×10^{-3}		1.8×10^{-2}	

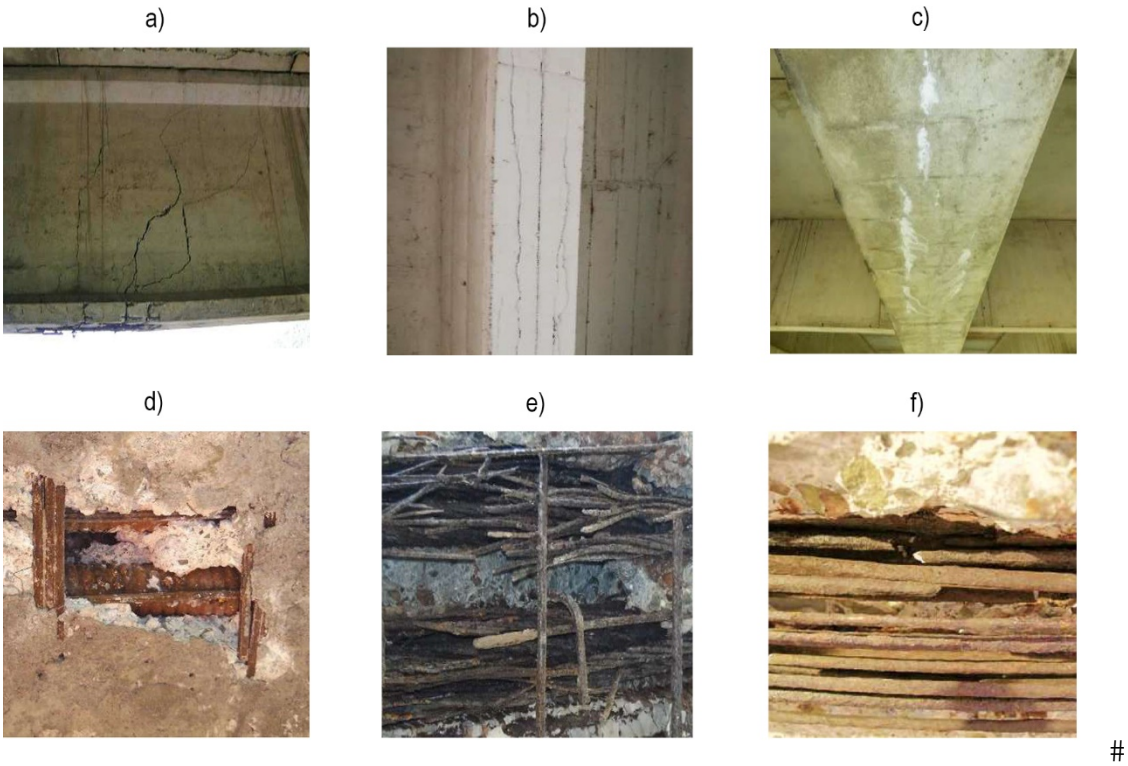

#

Figure 1. Damage phenomena in PC bridges: a) transverse cracks, b) longitudinal cracks, c) traces of humidity with efflorescence on the intrados, d) cavity located on the intrados, e) cables with strands interrupted at the intrados, f) corroded and broken wires.

Figure 2. a) General view of the viaduct, b) bottom view of the deck.

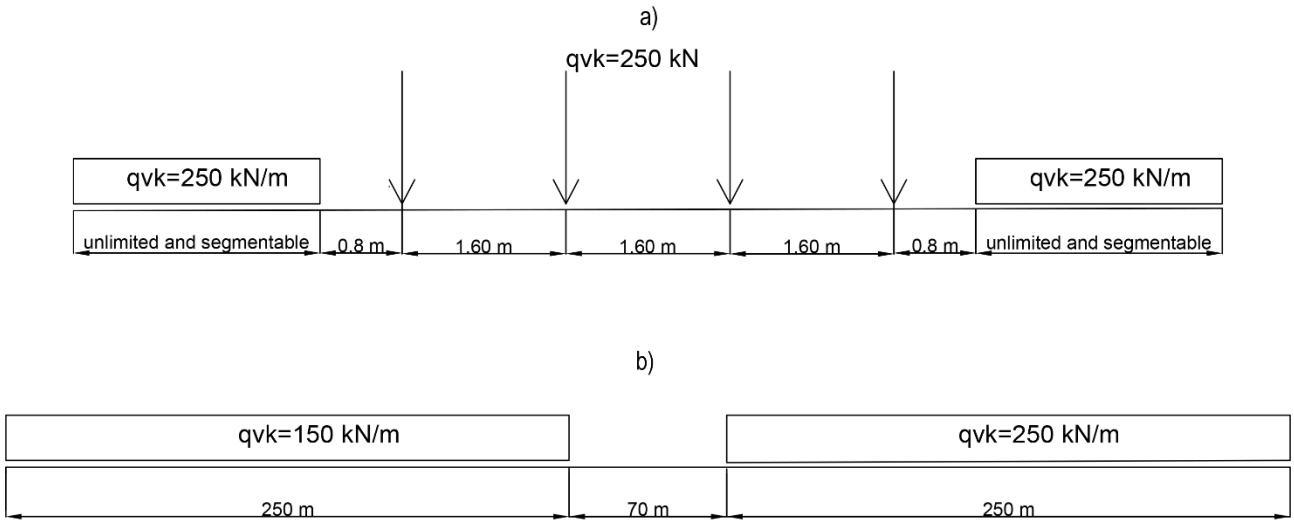

Figure 3: Design live loads: a) LM71, b) SW/2.

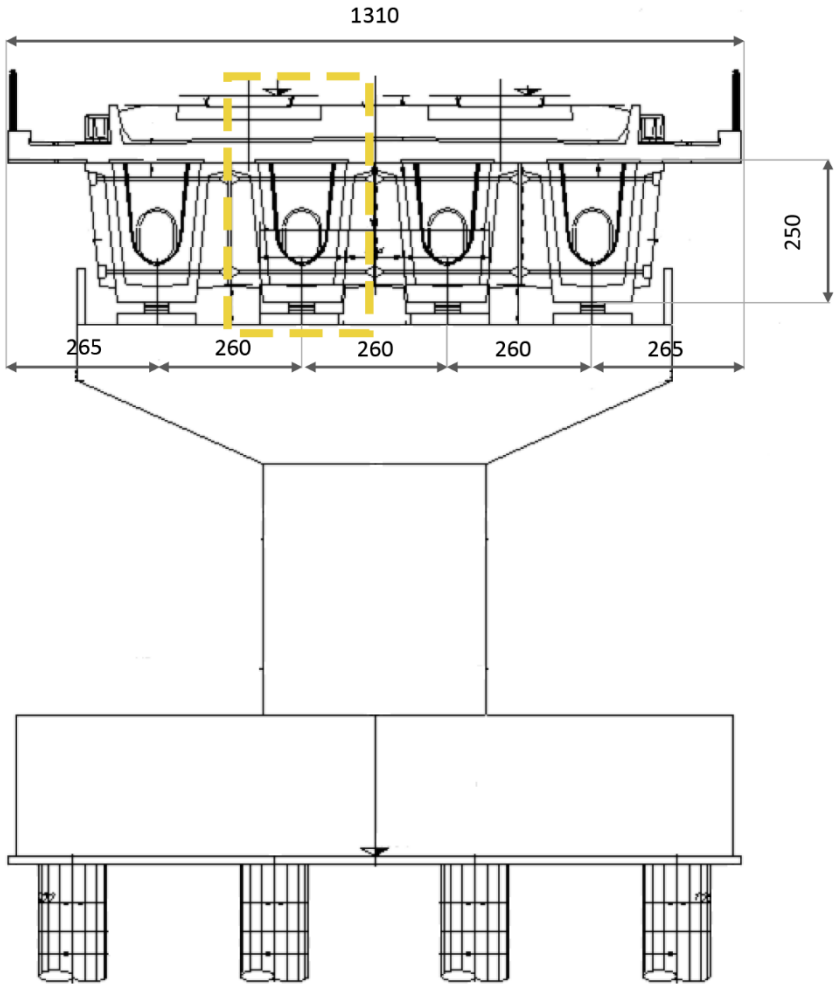

Figure 4. Pile elevation and bridge cross-section with indication of considered beam (dimensions in centimeters).

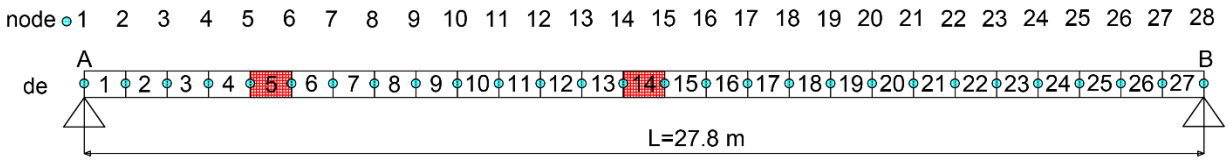

Figure 5. Simply-supported beam discretized by 27 elements. Red color identifies a generic couple of damaged elements.

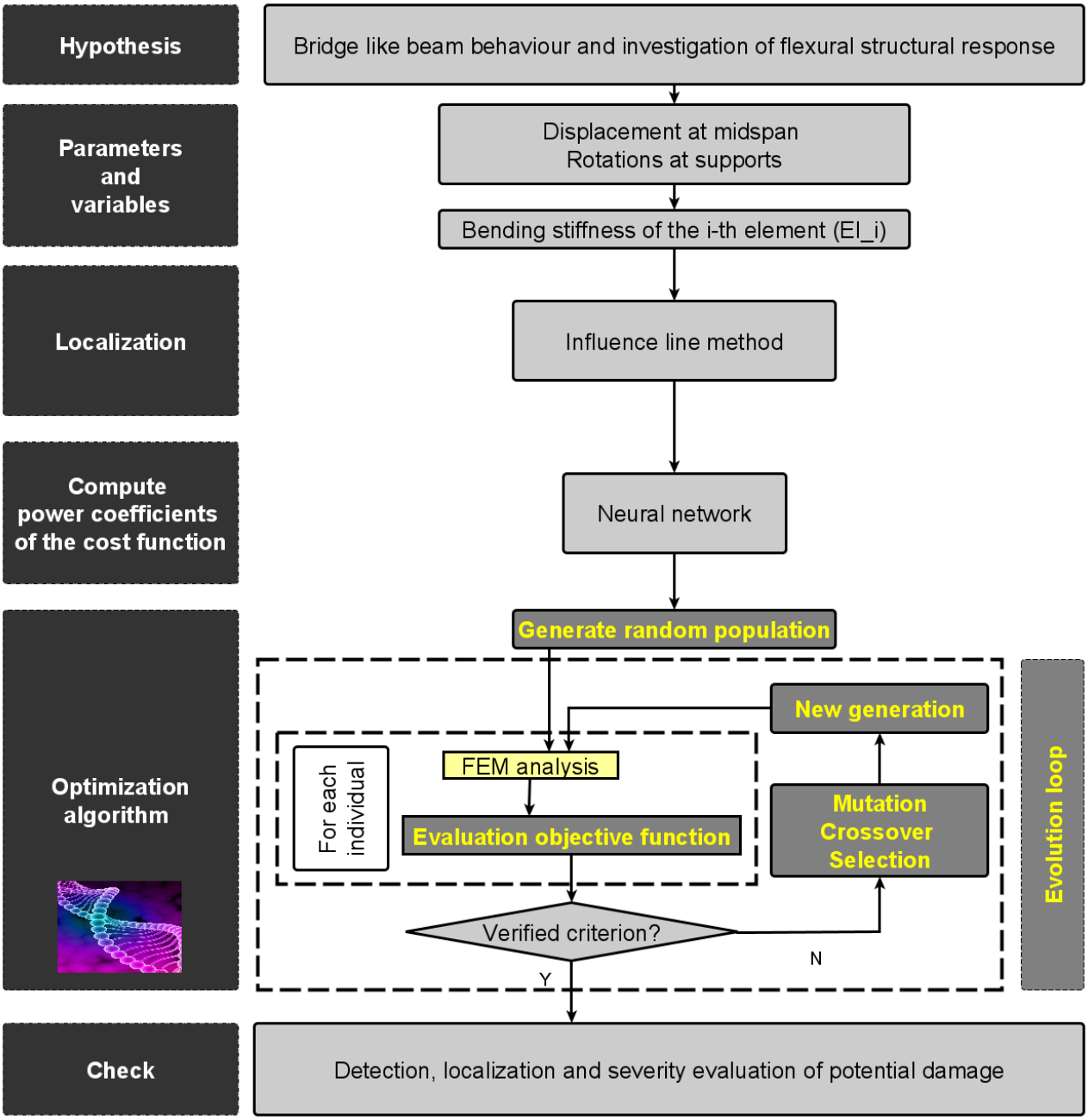

Figure 6. Flowchart of damage identification process.

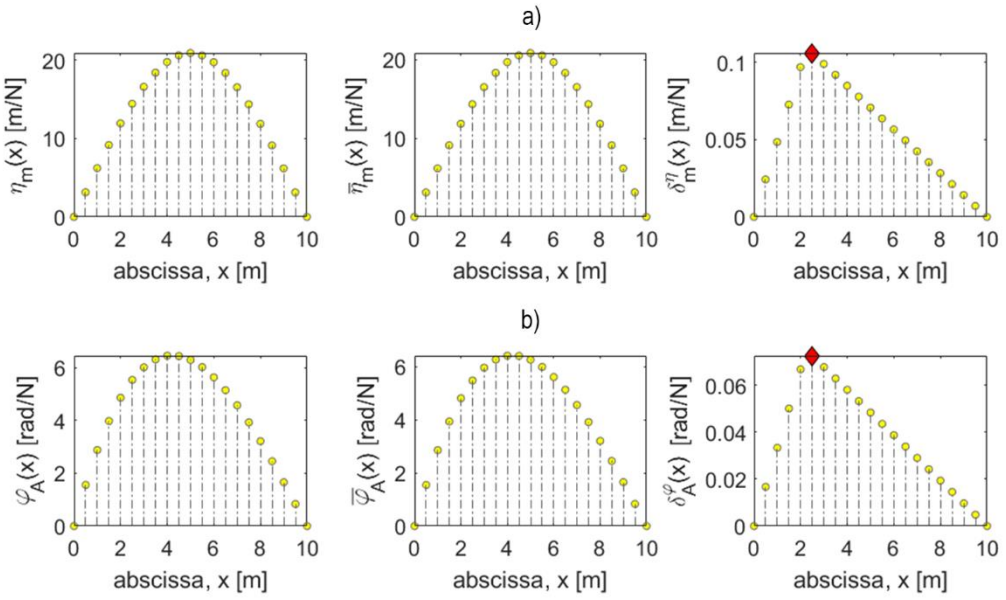

Figure 7. Damage identification by influence line method: illustrative example. a) mid-span deflection, b) left-support rotation.

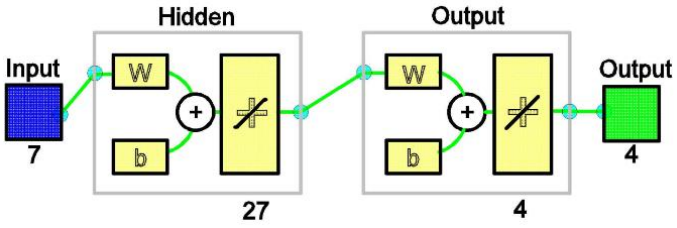

Figure 8. Neural network architecture.

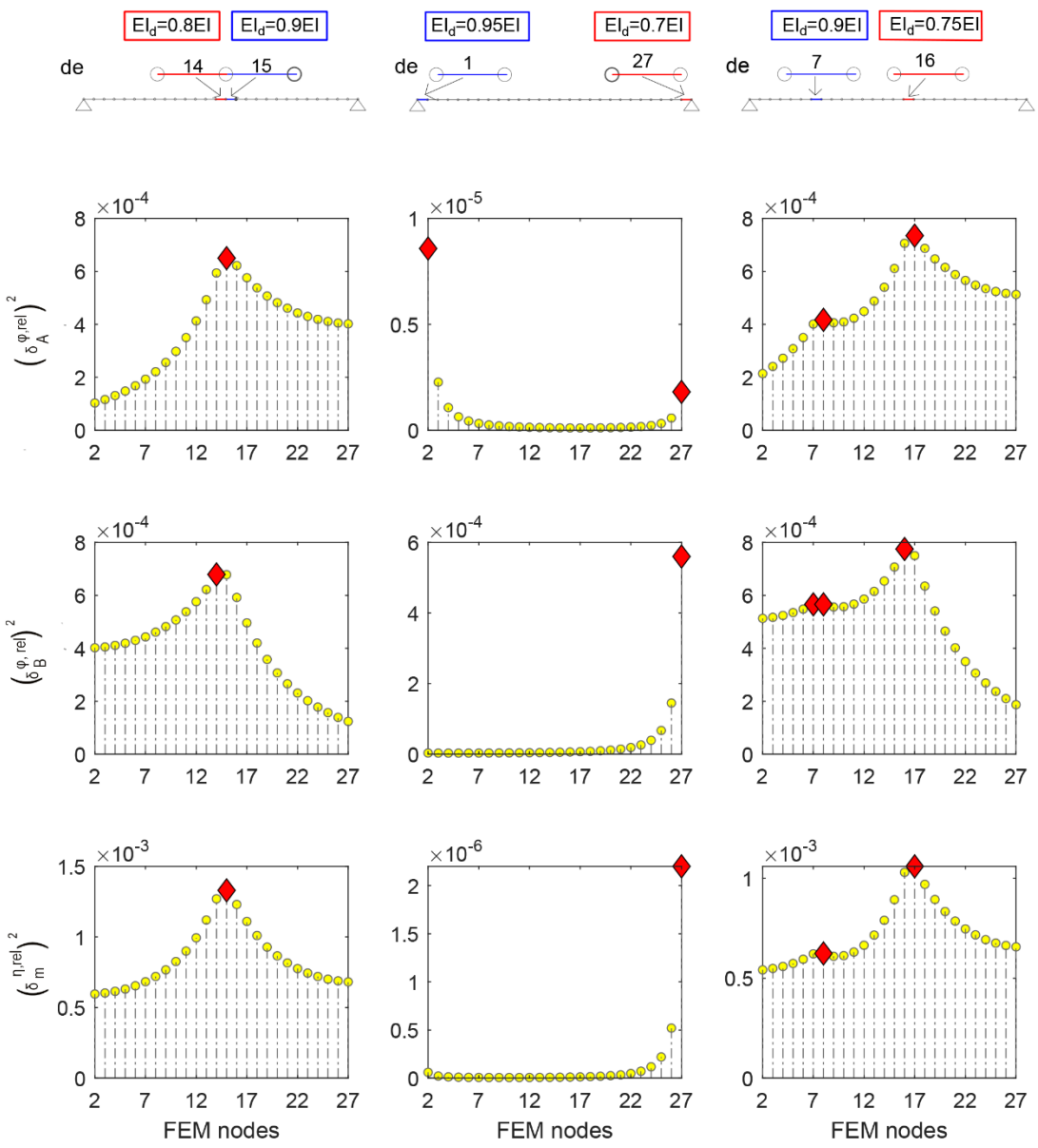

Figure 9. Three damage scenarios identified by influence line method.

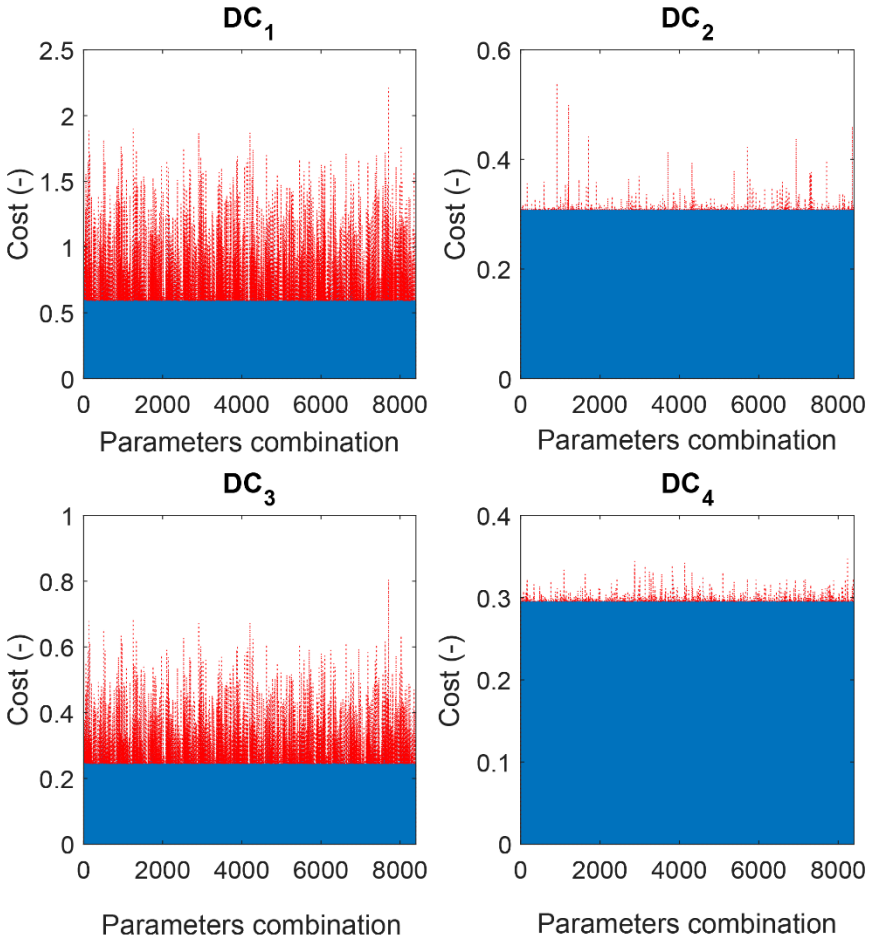

Figure 10. Cost as a function of the combinations of parameters and damage scenarios.

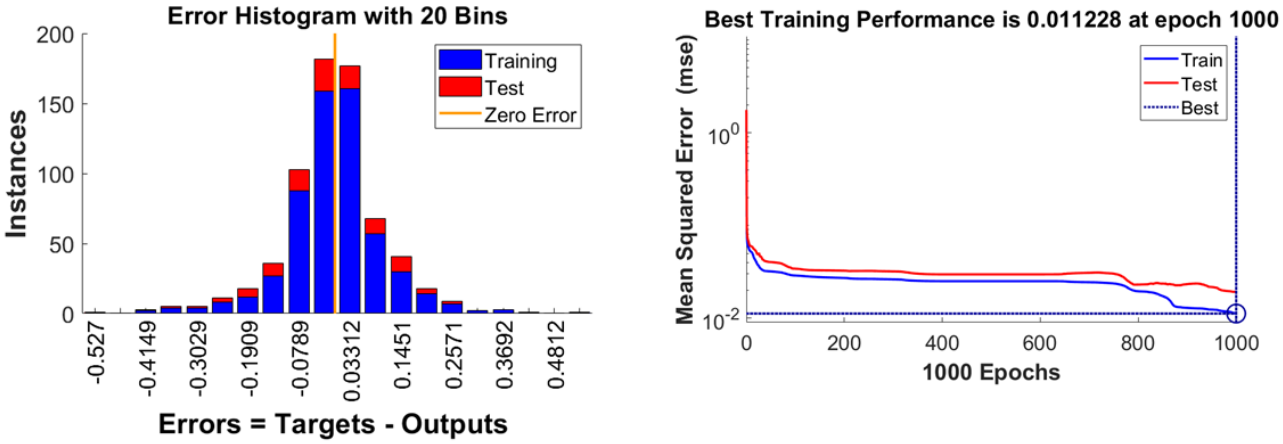

Figure 11. Error histogram and performance of neural network.

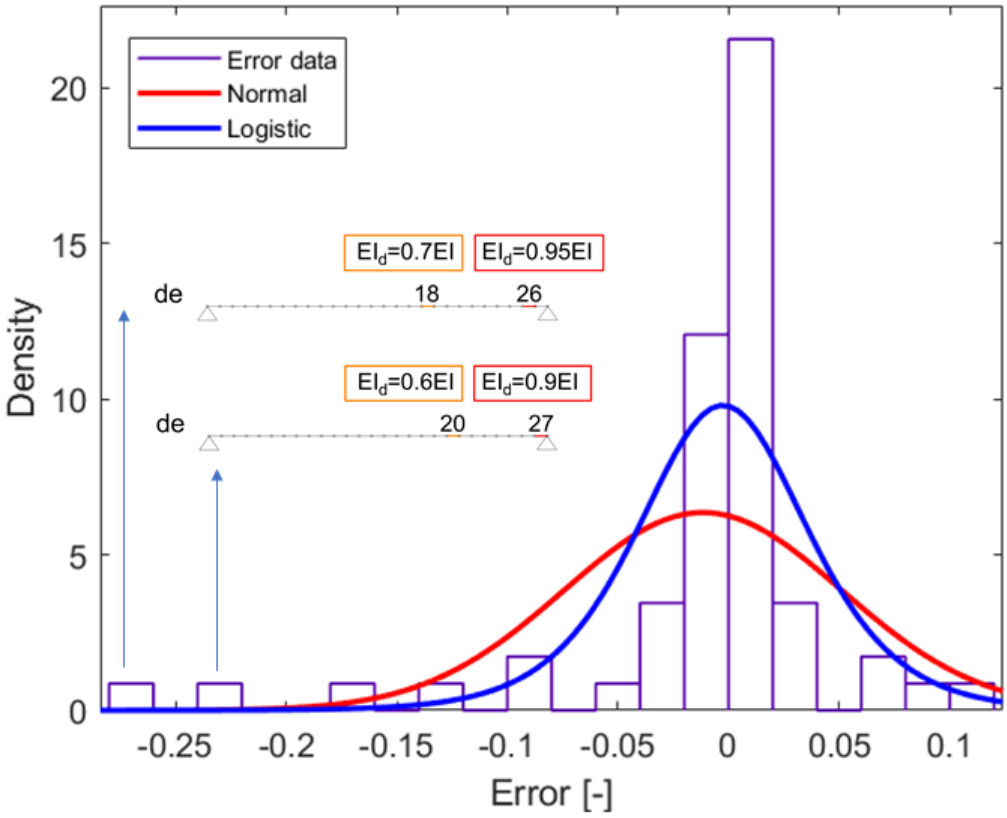

Figure 12. Distribution of the errors.